Chem Rev Lett 8 (2025) 751-763

Research Article

Chemical Review and Letters
journal homepage: www.chemrevlett.com
ISSN (online): 2645-4947 (print) 2676-7279

Effect of chitosan content on the adsorptive properties of activated carbon/chitosan composites toward rhodamine B

Dahlena Ariyani[1,2,*], Andre Firman Agustiansyah[2], Umi Baroroh Lili Utami[1], Utami Irawati[1], Ahmad Budi Junaidi[1]

[1]*Department of Chemistry, Faculty of Mathematics and Natural Sciences, Universitas Lambung Mangkurat, Jl. A. Yani Km 36, Banjarbaru, Kalimantan Selatan, Indonesia.*
[2]*Laboratory of Biomaterial Chemistry, Faculty of Mathematics and Natural Sciences, Universitas Lambung Mangkurat, Jl. A. Yani Km 36, Banjarbaru, Kalimantan Selatan, Indonesia.*

ARTICLE INFO

Article history:
Received 16 June 2025
Received in revised form 8 July 2025
Accepted 19 July 2025
Available online 30 July 2025

Keywords:
Activated carbon/chitosan composite; adsorption; rhodamine B

ABSTRACT

This study investigates the effect of chitosan content on the synthesis, physicochemical properties, and adsorption performance of activated carbon/chitosan composites for the removal of Rhodamine B (RhB) dye from aqueous solution. This study aims to determine the characteristics, including functional groups, moisture content, and stability of activated carbon/chitosan composites, as well as to obtain data on the ability of activated carbon/chitosan composites in adsorbing RhB. Activated carbon/chitosan composites were prepared with varying weight ratios of activated carbon to chitosan (8:2, 8:4, 8:6, and 8:8) and characterized using Fourier-Transform Infrared (FTIR) spectroscopy, UV-Vis spectrophotometer, and Scanning Electron Microscope (SEM). FTIR results confirmed the successful incorporation of chitosan onto the activated carbon matrix through hydrogen bonding and functional group interactions. Increasing chitosan content enhanced the presence of polar groups but led to decreased surface area and pore accessibility. The adsorption studies revealed that the composites achieved equilibrium within 60 minutes, with maximum adsorption observed at neutral pH. Adsorption data were best fitted by the Langmuir isotherm model, with maximum adsorption capacities of 71.41, 49.01, 41.84, and 37.59 mg/g for composites with increasing chitosan content, respectively. The data shows that while chitosan introduces functional sites favorable for dye interaction, excessive loading may hinder adsorption due to pore blockage.

1. Introduction

The release of synthetic dyes from industrial effluents has emerged as a critical environmental concern due to their persistence, toxicity, and resistance to conventional degradation processes. Among the various industrial sectors, the textile, paper, and plastic industries are the predominant sources of dye-contaminated wastewater [1], [2]. Rhodamine B (RhB), a xanthene-based cationic dye, is extensively employed due to its high stability and vivid coloration. However, it is recalcitrant to biodegradation and poses considerable ecotoxicological risks to aquatic ecosystems and human health [3], [4]. Consequently, the efficient removal of RhB from aqueous environments is imperative prior to discharge.

Numerous physical, chemical, and biological techniques have been investigated for dye removal, including photodegradation [5]–[8], ion exchange [9]–[11], oxidation [12], [13], membrane separation [14]–[16], and adsorption [3], [17], [18]. Among these, adsorption is widely regarded as one of the most promising approaches due to its simplicity, cost-effectiveness, and high efficiency in removing a broad range of dye molecules [19], [20]. Materials used as adsorbents must be environmentally

* Corresponding author; e-mail: dariyani@ulm.ac.id
https://doi.org/10.22034/crl.2025.530563.1634

friendly and able to adsorb dyes well. Activated carbon, owing to its high surface area, porosity, and well-developed pore structure, has been extensively utilized as an adsorbent in dye removal applications [4], [21]–[23]. The primary mechanism of dye uptake by activated carbon is physisorption, governed by Van der Waals interactions, while rapid and reversible, may also result in limited adsorption selectivity and stability under varying environmental conditions [18], [24]–[27].

To address the limitations of pristine activated carbon, recent studies have explored the development of composite adsorbents incorporating biopolymers such as chitosan. Chitosan, a naturally abundant and biodegradable polysaccharide derived from chitin, possesses functional amino and hydroxyl groups that facilitate stronger electrostatic and hydrogen bonding interactions with dye molecules [18], [28], [29]. In addition, chitosan is biodegradable, non-toxic, and environmentally friendly, rendering it a sustainable candidate for wastewater treatment applications [30], [31].

Activated carbon/chitosan composite is a promising alternative as an adsorbent in treating wastewater containing dyes such as RhB. However, the effectiveness of this composite is highly influenced by the effectiveness of the adsorbent. However, the performance of such composites is significantly influenced by synthesis parameters, particularly the chitosan content. An optimal chitosan dosage is essential to maximize adsorption capacity, as both under- and over-functionalization can detrimentally impact composite structure and dye uptake performance.

In this study, we investigate the effect of varying chitosan dosage on the adsorption performance of activated carbon/chitosan composites toward RhB removal. The objective is to determine the optimal chitosan concentration that enhances adsorption efficiency, thereby advancing the development of high-performance, sustainable adsorbents for the treatment of dye-laden industrial effluents.

2. Materials and Methods

2.1. Materials and tools

The materials used in this study were chitosan powder from Food Grade and Medical Grade shrimp skin (with moisture content 12.0% max, ash content 1.0% max, protein content 1.0% max, DAC 70% min, molecular weight 50,000-80,000), activated carbon (Merck) (with particle size < 100 µm), NaOH, 32% HCl, 100% glacial acetic acid (E.Merck), rhodamine B, aluminum foil, distilled water, and Whatman No. 42 filter paper.

The tools used are analytical balance (Ohaus), glassware such as goblets, watch glass, glass stirrer, erlenmeyer, measuring flask, volume pipette, stirring rod, funnel, dropper pipette, glass bottle, glass bottle, GKL 3005 shaker, pH meter (DrGray), spray bottle, oven (Thermologic), analytical instruments such as Shimadzu 8201PC Fourier Transform Infrared (FTIR) spectrophotometer, Scanning Electron Microscope (SEM) and Genesys 10v UV-Vis spectrophotometer.

2.2. Preparation of activated carbon/chitosan composite

Activated carbon/chitosan composites were synthesized through a simple blending and gelation process. Commercially available activated carbon (sieved to 100 mesh) was employed as the primary adsorbent matrix, while a 2% (w/v) chitosan solution was prepared by dissolving chitosan in dilute acetic acid under constant stirring. To evaluate the effect of chitosan dosage on the composite properties, four formulations were prepared by varying the weight ratio of activated carbon to chitosan (w/w) as follows: 8:2, 8:4, 8:6, and 8:8. The required mass of chitosan was calculated and converted into its corresponding volume of 2% solution to maintain the designed ratios.

The activated carbon was gradually added to the chitosan solution and stirred vigorously to ensure homogeneity. Subsequently, a 0.5 M NaOH solution was introduced in a 1:1 volume ratio with respect to the chitosan solution, inducing gelation through neutralization and precipitation of chitosan. The resulting activated carbon/chitosan gel was allowed to age for 24 hours at ambient temperature to stabilize the structure.

Following gelation, the composites were repeatedly washed with distilled water until a neutral pH was attained. The washed composites were then oven-dried at 60 °C for 24 hours and subsequently ground and sieved using a 70 mesh sieve to ensure particle uniformity, with the retained material collected from a 100 mesh sieve. The obtained composites were designated as CC82, CC84, CC86, and CC88, corresponding to the increasing chitosan content.

2.3. Preparation of rhodamine B (RhB) standard curve

A series of RhB standard solutions with concentrations of 1.5, 2.0, 2.5, 3.0, and 3.5 mg/L (ppm) were prepared by serial dilution of a stock RhB solution using deionized water. The absorbance of each solution was measured using a UV-Vis spectrophotometer at the maximum absorption wavelength of 554 nm. The resulting data were used to construct a calibration curve correlating absorbance

with RhB concentration.

2.4. Effect of contact time on rhodamine B adsorption on activated carbon/chitosan composites

To investigate the influence of contact time on dye adsorption, 0.5 g of the activated carbon/chitosan composite was introduced into 100 mL of a 100 ppm RhB solution in an Erlenmeyer flask. The suspension was agitated using a mechanical shaker for various time intervals: 5, 15, 30, 60, and 120 minutes. After each interval, the mixture was filtered using Whatman No. 42 filter paper. The absorbance of the resulting filtrate was recorded at 554 nm using a UV-Vis spectrophotometer to determine the residual RhB concentration.

2.5. Effect of pH on the ability of activated carbon/chitosan composite to adsorb rhodamine B dye

To assess the impact of pH on adsorption performance, 200 mL of 100 ppm RhB solution was adjusted to acidic, neutral, and alkaline pH values using dilute HCl or NaOH. The solution was divided into two portions: one served as a control, while 0.5 g of the activated carbon/chitosan composite was added to the other. The mixtures were stirred for the previously determined optimum contact time. Following treatment, the solutions were filtered using Whatman No. 42 filter paper, and the absorbance of the filtrate was measured at 554 nm using a UV-Vis spectrophotometer.

2.6. Determination of the adsorption capacity of rhodamine B on activated carbon/chitosan composite

Prepare RhB solution at optimum pH with initial concentration variations of 50, 100, 150, 200, and 250 ppm, then add 0.1 gram of composite and shake for optimum contact time. The activated carbon/chitosan composite and filtrate were separated using Whatman No. 42 filter paper, and then the absorbance was measured using a UV-Vis spectrophotometer.

3. Results and Discussion

3.1. Preparation of activated carbon/chitosan composites

The composite is a mixture of two materials, namely 100 mesh activated carbon and 2% chitosan solution in acetic acid. Activated carbon/chitosan composites were successfully synthesized with varying weight ratios of activated carbon to chitosan: 8:2, 8:4, 8:6, and 8:8 (w/w), designated as CC82, CC84, CC86, and CC88, respectively. his variation aimed to identify the optimum chitosan content that balances surface area with the presence of functional groups favorable for dye adsorption.

Activated carbon inherently possesses a variety of surface functional groups, including acidic groups such as carboxyl, neutral groups like phenolic hydroxyl, epoxy, and ether, as well as basic groups such as carbonyl and quinone [34], [35]. hese functional moieties enable a range of interactions with adsorbates, including electrostatic attraction, dipole–dipole interactions, Van der Waals forces, and hydrogen bonding. When chitosan is incorporated, additional amino and hydroxyl groups are introduced, further enhancing the composite's capacity for chemical interaction with dye molecules such as RhB.

Macroscopic observations indicated that increasing chitosan content enhanced the gel-like consistency of the composite during synthesis, suggesting successful interaction between the polymer matrix and the activated carbon. Subsequent drying yielded stable, solid composites that were easily ground and sieved to uniform particle sizes. These physical characteristics provide preliminary evidence of successful composite formation. Further evidence of functional group presence and surface morphology is explored through FTIR and SEM characterization in the following sections.

The surface of activated carbon still has some acidic functional groups such as carboxyl, neutral functional groups (phenolic OH, epoxy, and ether), and basic functional groups (carbonyl and quinone) [34], [35]. These functional groups allow the formation of electrostatic, dipole-dipole, Van der Waals, and hydrogen bond interactions with amine and hydroxyl groups on chitosan to form a composite.

3.2. Characterization of functional groups of activated carbon-chitosan composites using Fourier Transform Infrared (FTIR)

The FTIR spectrum of chitosan (Figure 2a) shows broad absorption band due to O–H and N–H stretching vibration at around 3342 cm^{-1}. A peak at 2867 cm^{-1} is attributed to aliphatic C–H stretching, while the band at 1024 cm^{-1} is characteristic of C–O stretching vibration typically found in functional groups such as alcohol and ethers. The FTIR spectrum of activated carbon (Figure 2b) present an absorption band at 3342 cm^{-1}, indicating the presence of surface hydroxyl (–OH) groups. The peak at 1582 cm^{-1} is attributed to aromatic C=C stretching, while the band at 1022 cm^{-1} corresponds to C–O stretching vibrations, reflecting the presence of oxygen-containing functional groups on the activated carbon surface.

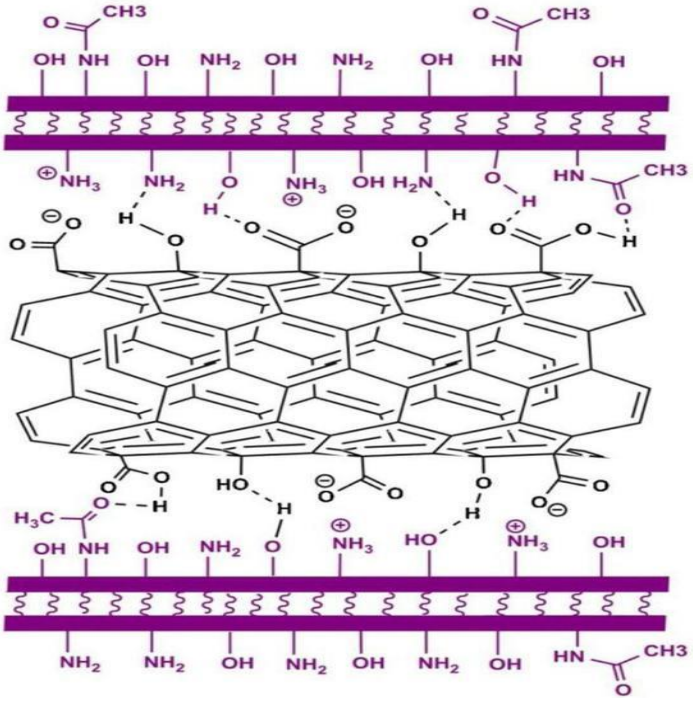

Fig. 1. Interaction between activated carbon and chitosan [32][33].

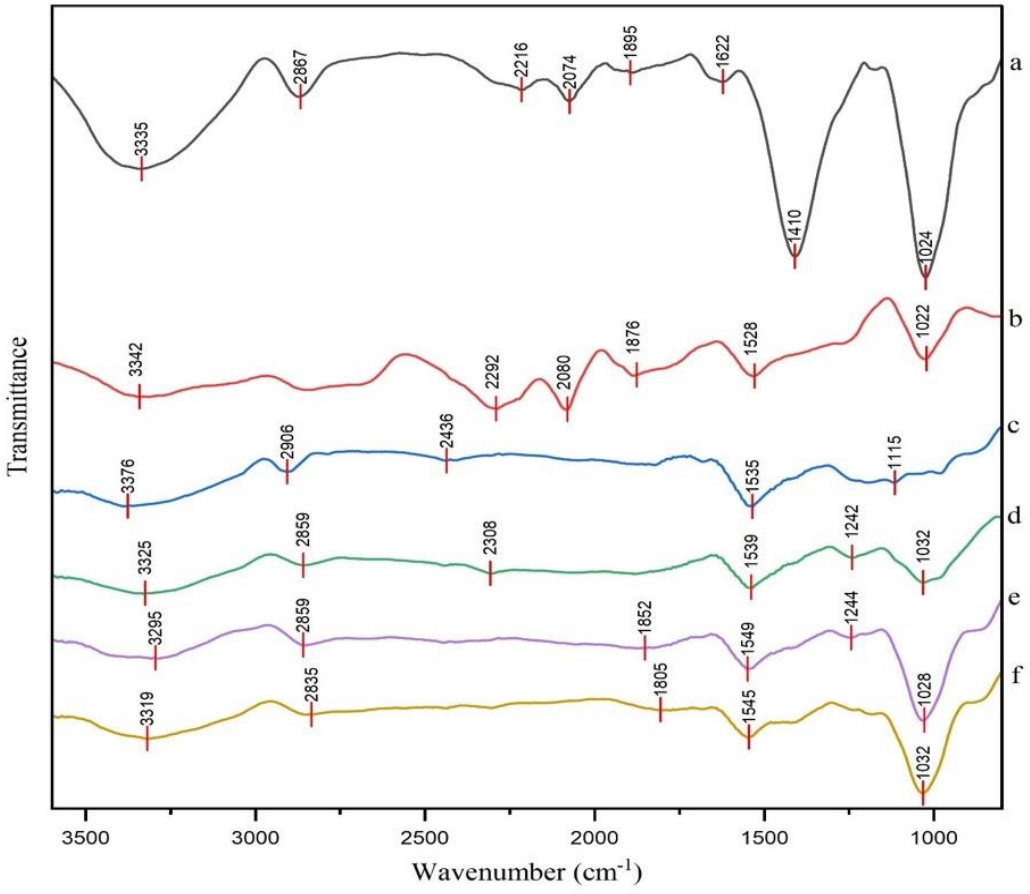

Fig. 2. FTIR spectra (a) chitosan, (b) activated carbon, (c) CC8:2, (d) CC8:4, (e) CC8:6, and (f) CC8:8

The FTIR spectra of the activated carbon/chitosan composites show broad bands at 3376 cm^{-1} (Figure 2c), 3326 cm^{-1} (Figure 2d), 3295 cm^{-1} (Figure 2e), and 3319 cm^{-1} (Figure 2f), which are attributed to O–H and N–H stretching vibrations. The reduced intensity of these bands suggests interactions between chitosan and activated carbon, confirming the successful formation of the composite. Furthermore, a significant shift to lower wavenumbers in the O–H/N–H stretching vibrations from 3342 cm^{-1} in pure chitosan to lower wavenumbers in the composites indicates enhanced hydrogen bonding between the functional groups of chitosan and the surface of activated carbon. The gradual shift observed at 3376, 3326, 3295, and 3319 cm^{-1} correlates with increasing chitosan content, suggesting that hydrogen bonding interactions become more prominent also likely increases the surface polarity and adsorption capacity. In Figure 2c, an absorption peak at 1535 cm^{-1} appears, which may be attributed to the interaction between aromatic C=C and amide groups of chitosan. The absorption band at 1115 cm^{-1} corresponds to C–O stretching vibrations, indicating the presence of oxygen-containing functional groups in the composite. The peaks at 1539 cm^{-1} and 1242 cm^{-1} in Figure 2d are attributed to C=C and C–N stretching vibrations, respectively, suggesting structural contributions from chitosan. The peaks at 1549 and 1028 cm^{-1} (Figure 2e), and at 1545 and 1022 cm^{-1} (Figure 2f), appear with greater intensity, indicating that C–O stretching vibrations become more prominent with increasing chitosan content..

3.3. Moisture content

Moisture content is the amount of water contained in the composite. The water content test was conducted using the gravimetric method by weighing the weight of the charcoal-chitosan composite before and after the water evaporated. The amount of water content can affect the absorbency of the composite; if the amount of water content is large, the pores of the composite will be filled with water and reduce the adsorption ability of the composite [36].

The activated carbon/chitosan composites used in this research contained a moisture content of 6.66–12.73% (Figure 3) and meet the requirements of SNI 06-3730-1995 regarding the quality of good activated carbon moisture content (moisture content <15%) [36]. An increasing trend in moisture content was observed with higher chitosan dosages in the composite formulations. This can be attributed to the hydrophilic nature of chitosan, which contains abundant polar functional groups such as $–NH_2$ and –OH that readily interact with and retain water molecules [30].

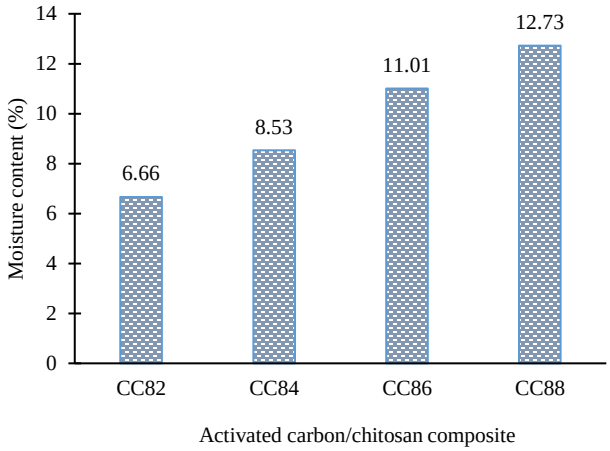

Fig. 3. Graph of the percentage of moisture content in activated carbon/chitosan composites with various ratios

3.4. Stability test of activated carbon/chitosan composite against acid solution

The acid stability of activated carbon/chitosan composites is a critical parameter, particularly due to the potential for protonation and deprotonation processes under varying pH conditions. In acidic conditions, the amine functional group on chitosan will protonate and form a $-NH_3^+$ group so that it is easily dissolved [37], [38]. The stability test in this study is based on analyzing the solubility of the activated carbon/chitosan composite in an acid solution. The greater the weight reduction of the composite after being dissolved in an acidic solution, the higher its solubility. This phenomenon indicates the lower the stability of the activated carbon/chitosan composite. Determination of composite stability was carried out by dissolving the composite in a pH 4 solution for 60 minutes. The results, as presented in Figure 4, indicate that all activated carbon/chitosan composites exhibited a reduction in mass after exposure to acidic conditions. However, the mass loss in all cases was less than 3%.

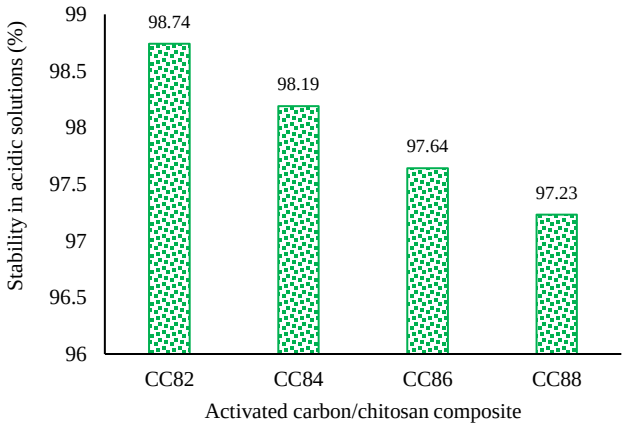

Fig. 4. Graph of percentage stability of activated carbon/chitosan composite in acid solution

The graph shows that the higher the dose of chitosan added in the preparation of activated carbon/chitosan, the lower the stability of the composite. It is suspected that the higher the dose of chitosan added, the more chitosan molecules are dissolved due to the nature of chitosan, which is easily soluble in acidic pH. However, the stability of the activated carbon/chitosan composite is still high, which can be caused by the interaction between the active groups on the activated carbon and the groups on the chitosan.

Nevertheless, in practical applications such as industrial wastewater treatment, the reduced stability of composites with higher chitosan content under acidic conditions may limit their long-term performance. To address this challenge, future improvements could include chemically crosslinking chitosan using agents like glutaraldehyde or epichlorohydrin to reduce solubility. These modifications could expand the applicability of the composite in acidic conditions.

3.5. Surface area test of activated carbon/chitosan composite

Determination of the surface area of the activated carbon/chitosan composite can be calculated through the methylene blue adsorption approach in an aqueous solution [39]. The equation used to calculate the surface area is

$$S = \frac{\frac{Ca}{m} \times N \times A}{Mr} \quad \dots (i)$$

with S as the adsorbent surface area (m^2/g), Ca as the amount of adsorbed dye (g), m is adsorbent weight (g), N is Avogadro's number (6.02 x 1023 particles/mol), A is the size of 1 molecule of methylene blue adsorbate (197 x 10-20 m^2/particle), Mr is the molecular weight of methylene blue (320.5 g/mol).

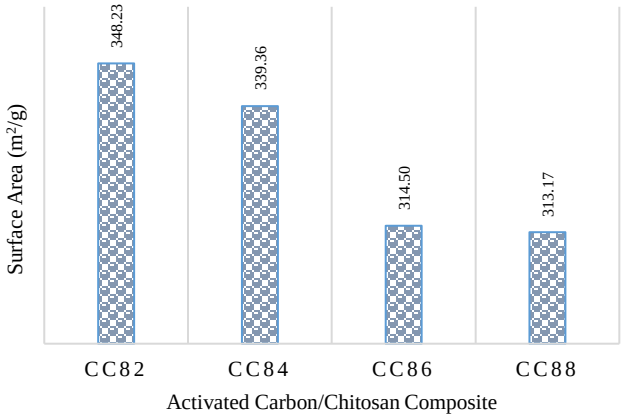

Fig. 5. Surface area graph of activated carbon/chitosan composite

Based on Figure 5, increasing the dosage of chitosan in the activated carbon/chitosan composite generally leads to a decrease in surface area, which can be caused by the filling of activated carbon pores by chitosan. The phenomenon is consistent with the surface morphology of the SEM analysis results. However, adding a higher dose of chitosan can improve the chemical adsorption properties through electrostatic interaction and covalent bond formation between activated carbon/chitosan composites as dye adsorbent. CC82 showed the highest surface area, indicating that activated carbon dominates the composite structure, keeping the pores open and easily penetrated by methylene blue molecules. The low dose of chitosan did not cover the pores on the activated carbon. The surface area of CC88 was only slightly lower than CC86, showing that adding chitosan no longer significantly impacted decreasing the surface area.

3.6. Surface morphology analysis based on SEM

SEM was employed to investigate the surface morphology and assess the influence of varying chitosan dosages on the structural features of the composite surface

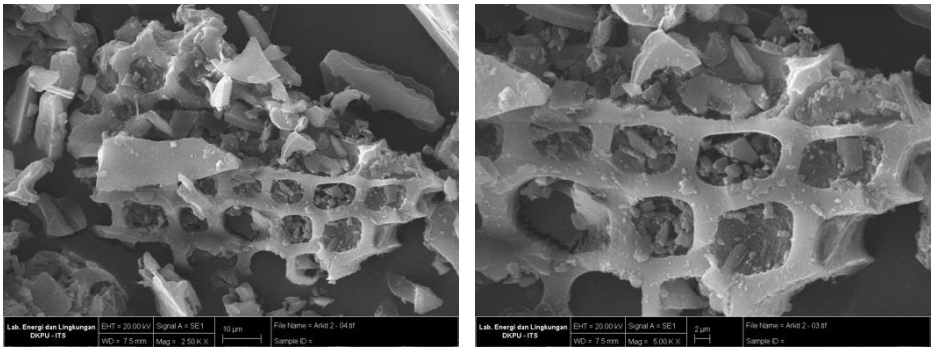

2500x 5000x

Fig. 6. Surface morphology of 8:2 ratio activated carbon/chitosan composite based on SEM analysis

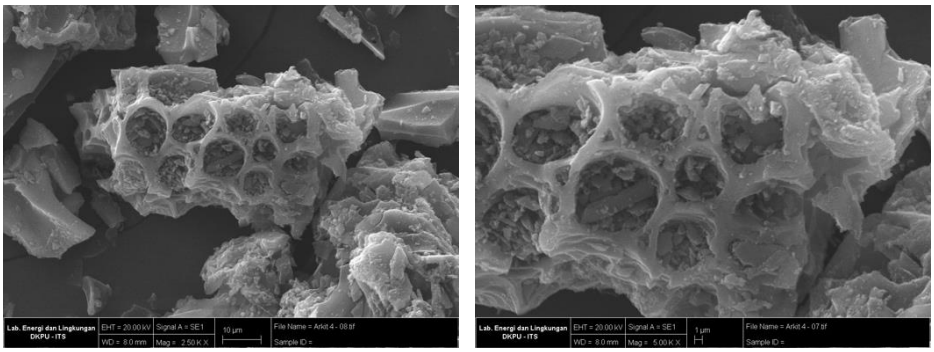

2500x 5000x

Fig. 7. Surface morphology of 8:4 ratio activated carbon/chitosan composite based on SEM analysis

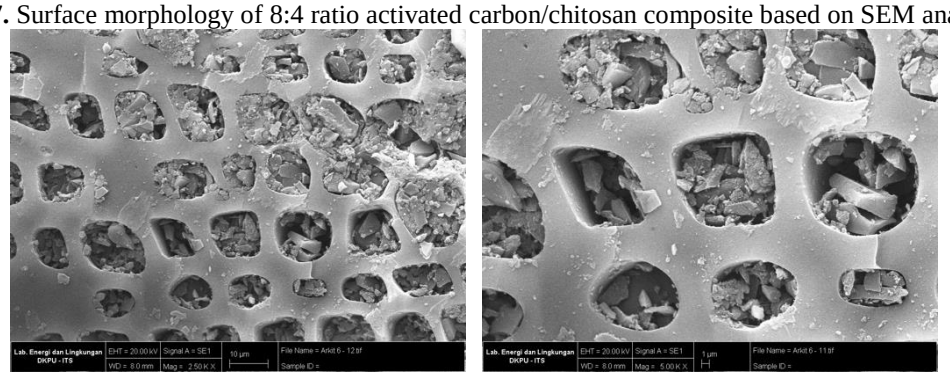

2500x 5000x

Fig. 8. Surface morphology of 8:6 ratio activated carbon/chitosan composite based on SEM analysis

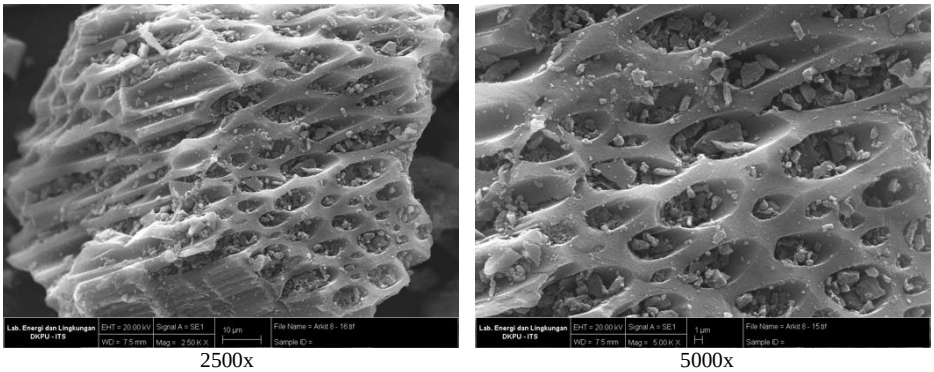

2500x 5000x

Fig. 9. Surface morphology of 8:8 ratio activated carbon/chitosan composite based on SEM analysis

The activated carbon/chitosan composite with a ratio of 8:2 in Figure 6 shows a relatively rough surface morphology and large pores. This result indicates the presence of activated carbon with a dominant macropore structure. At this lower chitosan content, the polymer does not significantly obstruct or fill the pores, resulting in visibly open and uncoated pore networks.

With the introduction of higher chitosan content (Figure 7), initial deposition of chitosan layers becomes apparent within the pore structure. As the chitosan dosage increases further (Figures 8 and 9), the surface becomes progressively smoother and the pore openings appear reduced. This suggests that chitosan begins to fill the internal voids of the activated carbon, partially masking the porous structure.

The gradual incorporation of chitosan significantly alters the composite's surface morphology. While increased chitosan content may reduce the accessible surface area due to pore blockage, it can enhance the composite's mechanical integrity and introduce more functional groups for chemical adsorption. Thus, the morphological transformation with increasing chitosan dosage reflects a trade-off between physical adsorption capacity and chemical interaction potential.

3.7. Effect of contact time on the adsorption of rhodamine B on activated carbon/chitosan composite

Figure 10 shows that the longer the contact time, the higher the adsorption percentage until it reaches equilibrium. The results showed that the percentage of RhB adsorption continued to increase with increasing contact time. The increase occurred at a contact time of 5-60 minutes, then after the 60 minute, there was no increase. These results indicate that the adsorbent has reached saturation point. Equilibrium conditions are reached because all active sides, pores, and functional groups on the composite have interacted with RhB to the maximum. The curve in Fig. 10 also shows that the higher the dose of chitosan added (chitosan activated carbon ratio), the longer the adsorption equilibrium is reached and the lower the adsorption percentage.

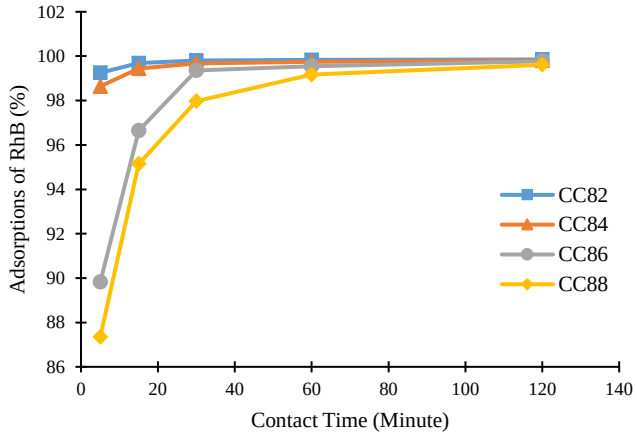

Fig. 10. Relationship curve between contact time and percentage adsorption of RhB dye on activated carbon/chitosan composite

3.8. Effect of pH on the ability of activated carbon/chitosan composite to adsorb rhodamine B dye

As shown in Figure 11, the adsorption efficiency of RhB by the activated carbon/chitosan composites is strongly influenced by the pH of the solution. The highest adsorption percentages were observed at neutral pH, particularly for composites CC84, CC86, and CC88. RhB is a cationic dye that contains a carboxyl group (–COOH), which can deprotonate to form –COO– at alkaline pH. RhB is a cationic dye containing a carboxyl group (–COOH), which can deprotonate to form –COO– in alkaline conditions. As a result, under acidic conditions, adsorption is predominantly facilitated by activated carbon, while the contribution of chitosan remains minimal due to its polycationic nature in such environments. Under neutral conditions, in addition to being in the form of cations, RhB also has carboxyl groups in the form of –COOH and –COO–, while the amine groups on chitosan can form $–NH_2$ and $–NH_3^+$ so that under these conditions, many interactions are likely to occur between the dye and the activated carbon/chitosan composite. In alkaline media, the amine groups of chitosan are predominantly deprotonated ($–NH_2$), reducing its positive charge and increasing the number of electronegative sites available for interaction. Although this may enhance electrostatic attraction with cationic RhB, the overall adsorption decreases slightly compared to neutral pH.

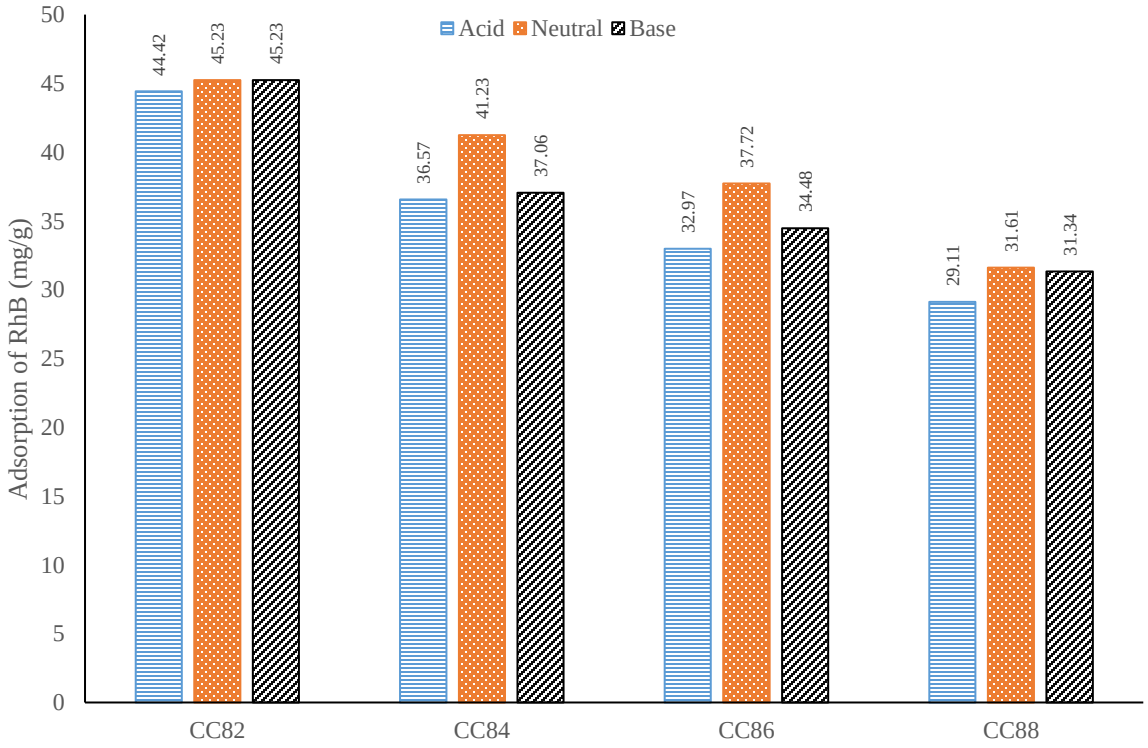

Fig. 11. Graph of the effect of pH on the percent adsorption of RhB on activated carbon/chitosan composites

In the case of CC82, the effect of pH variation on adsorption performance was negligible. This behavior is likely due to the predominance of activated carbon in the composite, where physisorption dominates via weak Van der Waals forces. Since the chitosan content is low, the availability of amine and hydroxyl groups that facilitate pH-dependent electrostatic or hydrogen bonding interactions is limited. Therefore, adsorption in CC82 is governed more by physical rather than chemical interactions, making it less responsive to changes in pH.

The higher the concentration of chitosan added to the manufacture of activated carbon/chitosan composites, the more amine groups will be present in the composite, and the adsorption process will be increasingly influenced by pH. These findings suggest that the adsorption of RhB onto the activated carbon/chitosan composite likely involves multiple mechanisms, primarily electrostatic interactions and hydrogen bonding. At neutral pH, the $–NH_2$ and –OH groups of chitosan may form hydrogen bonds with the polar functional groups of RhB, while the protonated $–NH_3^+$ groups can attract anionic RhB species through electrostatic attraction. Additionally, π–π interactions between the aromatic rings of RhB and the sp^2-hybridized carbon surfaces of activated carbon may further contribute to the overall adsorption process.

3.9. Determination of the adsorption capacity of rhodamine B (RhB) on activated carbon/chitosan composite

In general, the higher the concentration used, the greater the ability of the activated carbon/chitosan composite to adsorb RhB from the solution. The adsorption capacity of RhB by activated carbon/chitosan composite is determined using adsorption isotherm, which aims to determine the adsorption process that occurs on activated carbon/chitosan composite as adsorbent with RhB dye as adsorbate. The concentration of RhB solution can also affect the absorption rate until the activated carbon/chitosan composite can no longer absorb RhB due to the parallel relationship between concentration and the number of active sites present in activated carbon/chitosan in an equilibrium state.

Table 1. Calculation data of adsorption capacity of activated carbon/chitosan composite on rhodamine B

RhB (ppm)	Amount of adsorbed dye (qe) (mg/g)			
	CC82	CC84	CC86	CC88

50	10.36	10.38	10.39	10.25
100	21.22	21.22	21.21	21.23
150	30.02	29.95	29.92	28.67
200	37.03	36.52	34.84	33.63
250	47.50	46.75	45.06	36.68

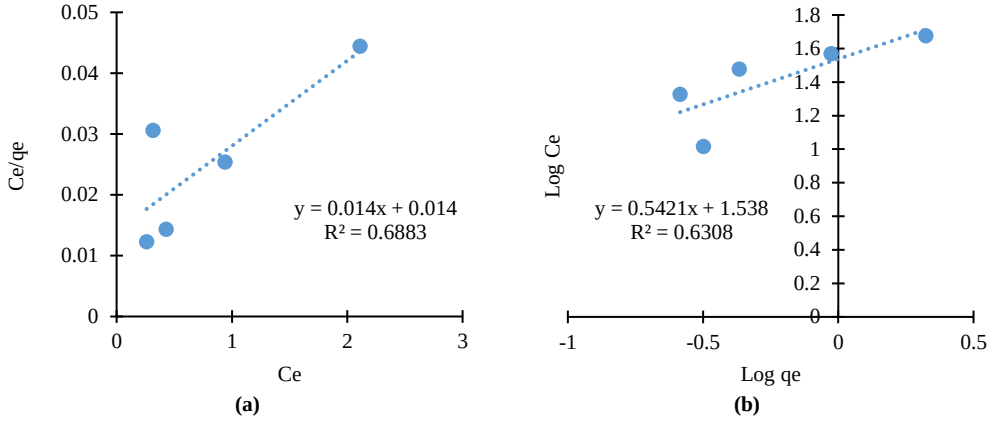

Fig.12. Results of (a) Langmuir and (b) Freundlich isotherm plots for 8:2 activated carbon/chitosan adsorption of RhB

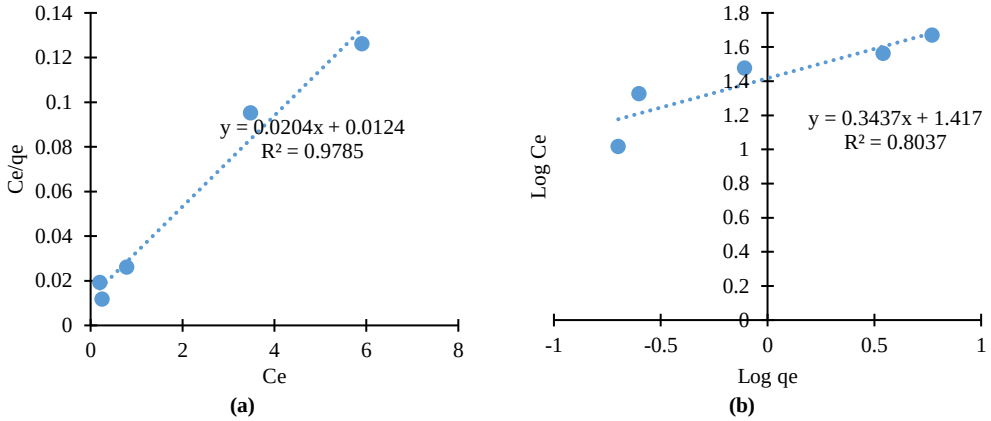

Fig. 13. Results of (a) Langmuir and (b) Freundlich isotherm plots for 8:4 activated carbon/chitosan adsorption of RhB

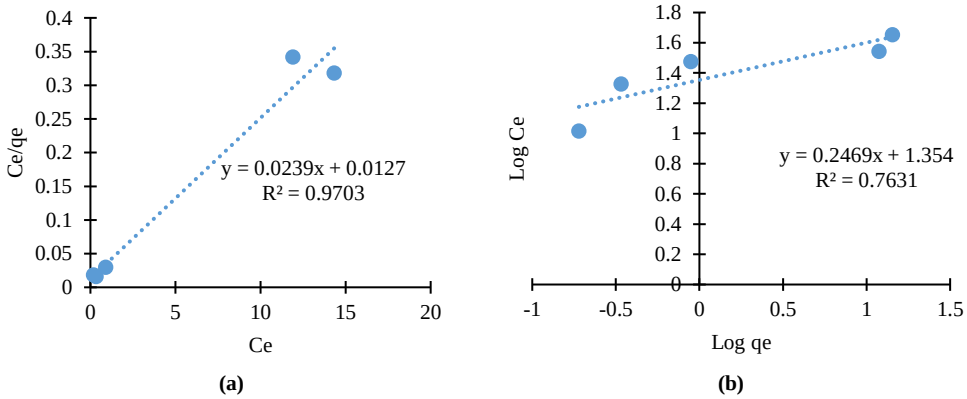

Fig. 14. Results of (a) Langmuir and (b) Freundlich isotherm plots for activated carbon/chitosan 8:6 adsorption of RhB

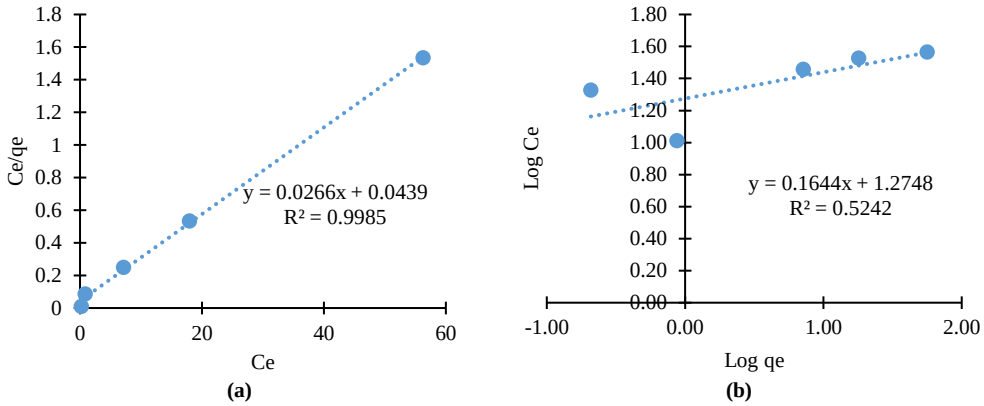

Fig. 15. Results of (a) Langmuir and (b) Freundlich isotherm plots for activated carbon/chitosan 8:8 adsorption of RhB

The plot indicates that the RhB adsorption isotherm pattern for activated carbon/chitosan composites with ratios of 8:2, 8:4, 8:6, and 8:8 tends to follow the Langmuir adsorption isotherm model. Evidence for this is provided by the R^2 value, which is closer to 1 compared to the R^2 value of the Freundlich adsorption isotherm model. The Langmuir adsorption isotherm model assumes that the dye only forms a single layer on top of a homogeneous adsorbent surface, which means that after one dye molecule occupies a site, no additional absorption will occur at that site.

For the activated carbon/chitosan 8:2 composite (CC82), both Langmuir (R^2 = 0.6883) and Freundlich (R^2 = 0.6308) models show relatively low correlation coefficients, indicating that neither model alone can adequately describe the adsorption behavior. This suggests that the adsorption mechanism in CC82 may involve a combination of physical and chemical interactions, possibly occurring over a heterogeneous surface with incomplete functionalization by chitosan. In contrast, composites with higher chitosan content, demonstrated better agreement with the Langmuir model (R^2 values > 0.9), suggesting that increased chitosan dosage enhances surface homogeneity and promotes monolayer adsorption behavior. This trend indicates that chitosan plays an important role in modifying the surface chemistry and adsorption characteristics of the composite. Interestingly, despite having the lowest chitosan content, the CC82 composite exhibited the highest surface area and also demonstrated relatively high adsorption capacity. This indicates that physical adsorption, likely driven by surface area, plays a more dominant role in RhB removal than chemical interactions. The lower chitosan dosage may have preserved the porous structure of activated carbon, allowing efficient diffusion and contact with RhB molecules, while still providing minimal functional groups for auxiliary interactions. In contrast, higher chitosan content may lead to partial pore blockage, reducing accessible surface area and thus lowering adsorption performance.

Table 2. Line equation data and R^2 for Langmuir and Freundlich adsorption isotherms of activated carbon/chitosan composites at various ratios

	Langmuir			Freundlich	
Composite	Line equation	q_{max} (mg/g)	R^2	Line equation	R^2
CC82	y= 0.0140x + 0.0140	71.42	0,6883	y= 0.5421x + 1.1538	0.6308
CC84	y= 0.0204x + 0.0124	49.01	0,9785	y= 0.3437x + 1.4170	0.8937
CC86	y= 0.0239x + 0.0127	41.84	0,9703	y= 0.2469x + 1.3540	0.7631
CC88	y= 0.0266x + 0.0493	37.59	0,9985	y= 0.1644x + 1.2748	0.5242

As shown in Table 2, increasing the chitosan dosage tends to reduce adsorption capacity, which may be attributed to partial pore blockage caused by excessive chitosan loading. This reduces the accessible surface area, despite the enhanced presence of functional groups such as –OH and –NH_2, as evidenced by stronger FTIR signals (e.g., more intense C–O stretching bands). These findings indicate that while chemical interactions such as hydrogen

bonding and electrostatic attraction are important, physical accessibility remains a key factor. Therefore, an optimal chitosan dosage is required to achieve a balance between surface functionality and pore accessibility for effective RhB adsorption.

In line with these considerations, it is also important to highlight the practical implications of composite performance, particularly in terms of reusability and regeneration. Although regeneration and reusability tests were not performed in this study, they represent critical parameters for evaluating the practical applicability of the composite adsorbent. Given the pH-sensitive nature of chitosan, alkaline desorption could serve as a promising regeneration method by weakening electrostatic and hydrogen bonding interactions with RhB. However, repeated exposure to high pH may degrade the structural integrity of the composite, particularly those with higher chitosan content. On the other hand, acidic desorption may enhance RhB release through protonation effects but may also lead to partial dissolution of chitosan. Therefore, careful optimization of desorption pH will be essential in future work to ensure a balance between regeneration efficiency and structural stability across multiple adsorption–desorption cycles.

4. Conclusions

Based on the characterization results in this study, activated carbon/chitosan composites have the potential to be used as dye adsorbents, especially rhodamine B (RhB). The optimum pH of RhB adsorption on activated carbon/chitosan composites occurred at neutral pH, especially on activated carbon/chitosan 8:4, activated carbon/chitosan 8:6, and activated carbon/chitosan 8:8, while on activated carbon/chitosan 8:2 composites the pH effect was not significant. The adsorption mechanism of RhB on the composite involves a combination of electrostatic attraction, hydrogen bonding, and π–π interactions, which are influenced by pH and chitosan content. The higher the initial concentration of RhB solution, the higher the adsorption ability of the activated carbon/chitosan composite. However, an inverse relationship was observed between chitosan content and adsorption capacity, as the proportion of chitosan in the composite increased, the overall adsorption capacity decreased. RhB adsorption onto activated carbon/chitosan composites follows the Langmuir isotherm model, with maximum adsorption capacities of 71.41, 49.01, 41.84, and 37.59 mg/g for composites with activated carbon to chitosan ratios of 8:2, 8:4, 8:6, and 8:8, respectively.

Acknowledgment

The authors would like to thank the Center for Research and Community Development of Universitas Lambung Mangkurat (Lembaga Penelitian dan Pengabdian kepada Masyarakat Universitas Lambung Mangkurat, LPPM ULM) for its generous financial support for this research.

References

[1] M.R. Islam and M. G. Mostafa, Textile dyeing effluents and environment concerns-a review. *J. Environ. Sci. Nat. Resour.*, 11 (2018) 131–144.

[2] L.A. Mokif, Removal methods of synthetic dyes from industrial wastewater: a review. *Mesopotamia Environ. J. (mesop. environ. j) ISSN 2410-2598*, 5 (2019) 23–40.

[3] Z.M. Saigl, Various adsorbents for removal of rhodamine b dye: A review. *Indones. J. Chem.*, 21 (2021) 1039–1056.

[4] W. Xiao, Z.N. Garba, S. Sun, I. Lawan, L. Wang, M. Lin, and Z. Yuan, Preparation and evaluation of an effective activated carbon from white sugar for the adsorption of rhodamine B dye. *J. Clean. Prod.*, 253 (2020) 119989.

[5] M. Roushani, M. Mavaei, A. Daneshfar, and H.R. Rajabi, Application of graphene quantum dots as green homogenous nanophotocatalyst in the visible-light-driven photolytic process. *J. Mater. Sci. Mater. Electron.*, 28 (2017) 5135–5143.

[6] H. R. Rajabi, F. Shahrezaei, and M. Farsi, Zinc sulfide quantum dots as powerful and efficient nanophotocatalysts for the removal of industrial pollutant. *J. Mater. Sci. Mater. Electron.*, 27 (2016) 9297–9305.

[7] H.R. Rajabi, H. Arjmand, H. Kazemdehdashti, and M. Farsi, A comparison investigation on photocatalytic activity performance and adsorption efficiency for the removal of cationic dye: quantum dots vs. magnetic nanoparticles. *J. Environ. Chem. Eng.*, 4 (2016) 2830–2840.

[8] H. R. Rajabi, F. Karimi, H. Kazemdehdashti, and L. Kavoshi, Fast sonochemically-assisted synthesis of pure and doped zinc sulfide quantum dots and their applicability in organic dye removal from aqueous media. *J. Photochem. Photobiol. B Biol.*, 181 (2018) 98–105.

[9] M. Constantin, I. Asmarandei, V. Harabagiu, L. Ghimici, P. Ascenzi, and G. Fundueanu, Removal of anionic dyes from aqueous solutions by an ion-exchanger based on pullulan microspheres. *Carbohydr. Polym.*, 91 (2013) 74–84.

[10] S. Raghu and C. A. Basha, Chemical or electrochemical techniques, followed by ion exchange, for recycle of textile dye wastewater. *J. Hazard. Mater.*, 149 (2007) 324–330.

[11] J. Joseph, R. C. Radhakrishnan, J. K. Johnson, S. P. Joy, and J. Thomas, Ion-exchange mediated removal of cationic dye-stuffs from water using ammonium phosphomolybdate. *Mater. Chem. Phys.*, 242 (2020) 122488.

[12] D. Peramune, D.C. Manatunga, R.S. Dassanayake, V. Premalal, R.N. Liyanage, C. Gunathilake, and N. Abidi, Recent advances in biopolymer-based advanced oxidation processes for dye removal applications: A review. *Environ. Res.*, 215 (2022) 114242.

[13] G. A. Ismail and H. Sakai, Review on effect of different

type of dyes on advanced oxidation processes (AOPs) for textile color removal. *Chemosphere*, 291 (2022) 32906.

[14] M. Liu, Q. Chen, and K. Lu, High efficient removal of dyes from aqueous solution through nanofiltration using diethanolamine-modified polyamide thin-film composite membrane. *Separation and Purification Technology*, 173 (2016).

[15] W. Chen, J. Mo, X. Du, Z. Zhang, and W. Zhang, Biomimetic dynamic membrane for aquatic dye removal. *Water Res.*, 151 (2019) 243–251.

[16] J. Lin, W. Ye, M.C. Baltaru, Y.P. Tang, N.J. Bernstein, O. Gao, S. Balta, M. Vlad, A. Volodin, A. Sotto, P. Luis, A.L. Zydney, and B.V. der Bruggen, Tight ultrafiltration membranes for enhanced separation of dyes and Na2SO4 during textile wastewater treatment. *J. Memb. Sci.*, 514 (2016) 217–228.

[17] M.M. Sabzehmeidani, S. Mahnaee, M. Ghaedi, H. Heidari, and V.A.L. Roy, Carbon based materials: a review of adsorbents for inorganic and organic compounds. *Cite this Mater. Adv*, 2 (2021) 598.

[18] L. Zhang, L. Sellaoui, D. Franco, G.L. Dotto, A. Bajahzar, H. Belmabrouk, Z. Li, Adsorption of dyes brilliant blue, sunset yellow and tartrazine from aqueous solution on chitosan: Analytical interpretation via multilayer statistical physics model. *Chem. Eng. J.*, 382 (2020) 122952.

[19] B.S. Rathi and P.S. Kumar, Application of adsorption process for effective removal of emerging contaminants from water and wastewater. *Environ. Pollut.*, 280 (2021) 116995.

[20] D. Lan, H. Zhu, J. Zhang, T. Wu, and M. Xu, Adsorptive removal of organic dyes via porous materials for wastewater treatment in recent decades: A review on species, mechanisms and perspectives. *Chemosphere*, 293 (2022) 133464.

[21] S. Husien, R.M. El-taweel, A. I. Salim, I.S. Fahim, L. A. Said, and A. G. Radwan, Review of activated carbon adsorbent material for textile dyes removal: Preparation, and modelling. *Curr. Res. Green Sustain. Chem.*, 5 (2022) 100325.

[22] K. Azam, N. Shezad, Y.K. Park, and M. Hussain, A review on activated carbon modifications for the treatment of wastewater containing anionic dyes. *Chemosphere*, 306 (2022) 135566.

[23] H. Wang, Z. Li, L. Sellaoui, and Q. Li, Effective adsorption of dyes on an activated carbon prepared from carboxymethyl cellulose: Experiments, characterization and advanced modelling. *Chem. Eng. J.*, 417 (2021) 128116.

[24] R. Ben-Mansour, M.A. Habib, O.E. Bamidele, and M. Ali, Carbon capture by physical adsorption: materials, experimental investigations and numerical modeling and simulations–a review," *Appl. Energy*, 161 (2016) 225–255.

[25] M. Sultana, M.H. Rownok, M. Sabrin, M.H. Rahaman, and S.M.N. Alam, A review on experimental chemically modified activated carbon to enhance dye and heavy metals adsorption. *Clean. Eng. Technol.*, 6 (2022) 100382.

[26] A.A. Abd, S.Z. Naji, A.S. Hashim, and M. R. Othman, Carbon dioxide removal through physical adsorption using carbonaceous and non-carbonaceous adsorbents: a review. *J. Environ. Chem. Eng.*, 8 (2020) 104142.

[27] M. Mariana, A. Khalil, E.M. Mistar, E.B. Yahya, T. Alfatah, M. Danish, and M. Amayreh, Recent advances in activated carbon modification techniques for enhanced heavy metal adsorption. *J. Water Process Eng.*, 43 (2021) 102221.

[28] I.O. Saheed, W. Da Oh, and F.B.M. Suah, Chitosan modifications for adsorption of pollutants: A review. *J. Hazard. Mater.*, 408 (2021) 124889.

[29] P.M. Morais da Silva, N. Camparotto, P. Prediger, Effective removal of basic dye onto sustainable chitosan beads: Batch and fixed-bed column adsorption, beads stability and mechanism. *Sustain. Chem. Pharm.*, 18 (2020) 100348.

[30] D. Ariyani, N.K. Hilma, U.B.L. Utami, U.T. Santoso, and D.R. Mujiyanti, Study Effect of Chitosan-Epichlorohydrin Macropore Beads on Decreasing the Value of Total Dissolved Solid (TDS) and Dyes in Sasirangan Liquid Waste Treatment. *Indo. J. Chem. Res.*, 11 (2023) 65–71.

[31] D. Ariyani, U.T. Santoso, and R. Nurmasari, Synthesis of Glutaraldehyde Crosslinked Superporous Chitosan with Polyvinyl Alcohol Addition for Peat Water Humic Acid Adsorption. *J. Wetl. Environ. Manag.*, 3 (2015) 79–89.

[32] M.J. Ahmed, B.H. Hameed, and E.H. Hummadi, Review on recent progress in chitosan/chitin-carbonaceous material composites for the adsorption of water pollutants. *Carbohydr. Polym.*, 247 (2020) 116690.

[33] R. Khakpour and H. Tahermansouri, Synthesis, characterization and study of sorption parameters of multi-walled carbon nanotubes/chitosan nanocomposite for the removal of picric acid from aqueous solutions. *Int. J. Biol. Macromol.*, 109 (2018) 598–610.

[34] M. Ai-qin, W. Hua, T. Ling-hua, and P. Renming, Research progress in characterization of functional groups on activated carbon. *Applied Chem. Ind.*, 40 (2011)1266.

[35] C. Qiu, L. Jiang, Y. Gao, and L. Sheng, Effects of oxygen-containing functional groups on carbon materials in supercapacitors: A review, *Mater. Des.*, 230 (2023) 111952.

[36] S. Maulina, G. Handika, I. Irvan, and A.H. Iswanto, Quality comparison of activated carbon produced from oil palm fronds by chemical activation using sodium carbonate versus sodium chloride. *J. Korean Wood Sci. Technol.*, 48 (2020) 503–512.

[37] J. Wang and S. Zhuang, Chitosan-based materials: Preparation, modification and application. *J. Clean. Prod.*, 355 (2022) 131825.

[38] Y. Yuan, W. Tan, J. Zhang, Q. Li, and Z. Guo, Water-soluble amino functionalized chitosan: Preparation, characterization, antioxidant and antibacterial activities. *Int. J. Biol. Macromol.*, 217 (2022) 969–978.

[39] N. Hegyesi, R.T. Vad, and B. Pukánszky, Determination of the specific surface area of layered silicates by methylene blue adsorption: The role of structure, pH and layer charge. *Appl. Clay Sci.*, 146 (2017) 50–55.